Surface Sol−Gel Synthesis of Ultrathin Semiconductor Films

Nina I. Kovtyukhova,*,† Eugenia V. Buzaneva,‡ Chad C. Waraksa,§ Benjamin R. Martin,§ and Thomas E. Mallouk§

Institute of Surface Chemistry, 31, Pr. Nauky, 252022 Kiev, Ukraine, Kiev T. Shevchenko University, 64, Vladimirskaya Str., 252033 Kiev, Ukraine, and The Pennsylvania State University, University Park, Pennsylvania 16802, USA

Received June 23, 1999. Revised Manuscript Received November 9, 1999

Ultrathin films of ZnS, Mn-doped ZnS, ZnO, and SiO_2 were grown on silicon substrates using surface sol−gel reactions, and the film growth process was characterized by ellipsometry, atomic force microscopy, X-ray photoelectron spectroscopy, UV−visible absorbance, and photoluminescence (PL) spectroscopy. The Si substrates were pretreated by chemical oxidation, or by derivatization with 4-((dimethylmethoxy)silyl)butylamine. On the oxidized Si/SiO_x surface, nanoparticulate films of ZnS and Mn-doped ZnS were grown by sequential immersion in aqueous metal acetate and sodium sulfide solutions. During the first four adsorption cycles, there was little film growth, but thereafter the amount of material deposited was linear with the number of adsorption cycles. This behavior is consistent with the formation of ZnS nuclei at low coverage, followed by particle growth in subsequent cycles. PL spectra are consistent with incorporation of Mn^{2+} into the ZnS nanoparticles. In contrast, the growth of SiO_2 films from nonaqueous $SiCl_4$ on the same Si/SiO_x substrates was regular from the first adsorption cycle, indicating a high density of nucleation sites. On amine-derivatized substrates, ZnO thin films grew as relatively smooth islands, suggesting that the interaction of Zn^{2+} ions or primary ZnO clusters with the amine surface priming layer was sufficiently strong to prevent the formation of isotropic nanoparticles upon exposure to aqueous base.

Introduction

There is growing interest in developing techniques for preparing ultrathin semiconductor nanoparticle films. This work is motivated by the size-dependent electronic and optical properties of semiconductors, which lead to a range of potential applications in electronic and optoelectronic devices, solar cells, photoelectrodes, photocatalysts, and sensors. The wet chemical synthesis of ultrathin semiconductor films represents, in principle, a simple and inexpensive alternative to more technologically demanding chemical vapor deposition (CVD) and physical techniques.[1−3] However, the realization of practical devices from wet chemical synthesis requires the development of film growth techniques that give similar or better quality films than vapor-phase methods. In particular, precise control of film thickness, crystallinity, and morphology are significant problems to be overcome in wet chemical synthesis.

There are essentially three strategies for preparing uniform films of semiconductor nanoparticles. One is by electrochemical deposition of a compound semiconductor, either directly from a solution containing both atomic components (e.g., Cd^{2+} and Se),[4] or by chemical reaction of a second component (chalcogen or halogen) with an electrodeposited layer of metal particles.[5] In favorable cases, particularly when there is a good epitaxial match between the substrate and the semiconductor lattice, well-crystallized films can be formed. The second method involves particle self-assembly, in which preformed colloidal particles are attached layer-by-layer to a growing surface film.[6−9] In this case, the quality of the film depends on the properties of the nanoparticles used, as well as the attachment chemistry. The third method, which potentially offers the finest control over the film growth process, is the direct layer-by-layer synthesis from the chemical components (e.g., anion and cation) of the semiconductor. The latter method typically involves a two-step chemisorption/

* Corresponding author.
† Institute of Surface Chemistry.
‡ Kiev T. Shevchenko University.
§ The Pennsylvania State University.

(1) Fendler, J. H.; Meldrum, F. *Adv. Mater.* **1995**, *7*, 607.
(2) Alivisatos, A. P. *MRS Bull.* **1998**, *23*, 2, 18.
(3) Mallouk, T. E.; Kim, H.-N.; Ollivier, P. J.; Keller, S. W. In *Comprehensive Supramolecular Chemistry*; Alberti, G., Bein, T., Eds.; Elsevier Science: Oxford, UK, 1996; Vol. 7, p 189.
(4) (a) Golan, Y.; Margulis, L.; Rubinstein, I.; Hodes, G. *Langmuir* **1992**, *8*, 749. (b) Golan, Y.; Margulis, L.; Hodes, G.; Rubinstein, I.; Hutchison, J. L. *Surf. Sci.* **1994**, *311*, L633. (c) Golan, Y.; Hodes, G.; Rubinstein, I. *J. Phys. Chem.* **1996**, *100*, 2220.
(5) (a) Hsiao, G. S.; Anderson, M. G.; Gorer, S.; Harris, D.; Penner, R. M. *J. Am. Chem. Soc.* **1997**, *119*, 1439. (b) Gorer, S.; Ganske, J. A.; Hemminger, J. C.; Penner, R. M. *J. Am. Chem. Soc.* **1998**, *120*, 9584.
(6) Iler, R. K. *J. Colloid Interface Sci.* **1966**, *21*, 569.
(7) Colvin, V. L.; Golstein, A. N.; Alivisatos, A. P. *J. Am. Chem. Soc.* **1992**, *114*, 5221.
(8) Kotov, N.; Dekany, I.; Fendler, J. *J. Phys. Chem.* **1995**, *99*, 13065.
(9) Ollivier, P. J.; Kovtyukhova, N. I.; Keller, S. W.; Mallouk, T. E. *Chem. Commun.* **1998**, 1563.

10.1021/cm990395p CCC: $19.00
Published on Web 01/15/2000

chemical activation cycle.[10−16] One component is adsorbed or reacted chemically with molecules on the surface, but the reaction is self-limiting at the extent of a single monolayer. The chemisorbed monolayer is then activated in the second step, by reaction with an appropriate reagent[11−13] or by redox reactions[15,16] in the liquid phase. Alternatively, the activation step may occur in a gas-phase process, such as UV ozone oxidation or low-temperature plasma treatment.[10,17−19]

When the third technique uses solution-phase activation of the surface, it is called the surface sol−gel (SSG) process.[12−14] SSG can be considered as both a surface variant of the bulk sol−gel method and a liquid-phase variant of the vapor-phase atomic layer epitaxy method (ALE).[20,21] A technique that is closely related to SSG and ALE is electrochemical atomic layer epitaxy (ECALE), in which either the adsorption or activation step is a Faradaic redox process.[14−16] SSG is based on self-limiting surface *chemical* reactions between the surface and each of the film components. The first examples of SSG involved the synthesis of semiconductor particles by alternate adsorption of anions and cations from aqueous solutions, and was called SILAR (successive ionic layer adsorption and reaction).[12] Later, Ichinose et al. generalized the technique to include molecular precursors, such as metal alkoxides, which could be adsorbed and hydrolyzed as monolayer films.[13] The process is experimentally simple, involving alternate immersion of the substrate in solutions of the components of a compound semiconductor. Each reaction step is followed by rinsing with the appropriate solvent to remove excess reagent. SSG combines the advantages of ALE and the bulk sol−gel method: it provides film thickness control at the Ångstrom level, and therefore allows one to tune the band gap and related properties through control of particle size. Like bulk sol−gel synthesis, SSG does not require high temperatures or expensive high-vacuum equipment. Another strong point of SSG is its compatibility with surface patterning techniques. This has been illustrated by the fabrication of patterned TiO_2 films on Si/SiO_2 substrates bearing microcontact-printed lines of an organic polysiloxane.[14] A distinct disadvantage is that as a low-temperature synthesis technique, SSG may give low-density or incompletely crystallized films. In a previous paper, we showed low density surface oxides made by SSG can be thermally annealed to give smooth, adherent, high-density thin films.[14]

To date the SSG method has been successfully applied to the synthesis of CdS, ZnS,[11,12] Ti, Zr, Al and B oxides,[13] and mixed Ti, Ta oxides[14] as thin films. The related ECALE technique has been used to make a variety of II−VI semiconductors.[15,16] In this work, we extend the SSG technique to the preparation of nanoparticle films of the wide-band-gap semiconductors ZnS, Mn-doped ZnS, and ZnO. SSG ZnS and SiO_2 films were also studied for comparison purposes. Our interest in ZnS and (Zn,Mn)S is motivated by their commercial use as phosphors and functional layers in electroluminescent and photovoltaic devices.[22−24] The oxides (ZnO and SiO_2) are also useful as insulating layers.[25] Further, a recent study has shown that certain silica sol−gels, in bulk form, are highly photoluminenscent.[26] As thin films, these organosilicate gels may also be interesting for electroluminescent display applications. We describe here the SSG synthesis of ultrathin ZnS, Mn-doped ZnS, ZnO, and SiO_2 films and their characterization by atomic force microscopy (AFM), X-ray photoelectron spectroscopy (XPS), ellipsometry, and UV−visible and photoluminescence (PL) spectroscopy.

Experimental Section

Materials. Zinc acetate dihydrate, $Zn(OAc)_2 \cdot 2H_2O$, manganese acetate tetrahydrate, $Mn(OAc)_2 \cdot 4H_2O$, sodium hydroxide, sodium sulfide nonahydrate, $Na_2S \cdot 9H_2O$, and carbon tetrachloride were purchased from Aldrich. Silicon tetrachloride was purchased from Acros. These compounds were used without further purification. Doubly distilled water was used in all experiments. Polished (100) Si wafers were obtained from Research and PVD Materials Company. All other chemicals were reagent grade, obtained from commercial sources, and used as received.

Film Synthesis. Si wafers were sonicated in CCl_4 for 15 min and then rinsed with 2-propanol and water. OH-terminated Si surfaces (Si−OH) were prepared by 30 min sonication in "piranha" solution (4:1 concentrated H_2SO_4:30% H_2O_2) and rinsed with copious amount of water. Ellipsometric data revealed the presence of a ∼2 nm thick SiO_2 film on the Si surface. An amine-terminated Si surface (Si∧∧NH_2) was prepared by washing Si−OH sequentially with methanol and 1:1 methanol/toluene and then reacting it with 4-((dimethylmethoxy)silyl)butylamine (15 h treatment with 5% toluene solution in dry argon over KOH at ambient temperature). Quartz slides, treated in the same way, were also used as substrates.

ZnS and Mn-doped ZnS (Zn,Mn)S films were prepared as follows. Si−OH substrates was placed in a beaker (for 5 min) in an aqueous solution of $Zn(OAc)_2$ (91 mM, pH 6.7) or a mixture (10 mL:0.2 mL, pH 6.74) of aqueous solutions of $Zn(OAc)_2$ (91 mM) and $Mn(OAc)_2$ (98 mM, pH 7.7), respectively. The substrates were then rinsed with water and dried in a stream of Ar. The substrates then were immersed in aqueous Na_2S solution (4 mM, pH 11.05) for 2 min, rinsed with water and dried in Ar. ZnO films were prepared by alternately

(10) Bruner, H.; Vallant, T.; Meyer, U.; Hoffmann, H. *Langmuir* **1996**, *12*, 4614.
(11) Vogel, R.; Rohl, K.; Weller, H. *Chem. Phys. Lett.* **1990**, *174*, 241.
(12) (a) Nicolau, Y. F. *Appl. Surf. Sci.* **1985**, *22/23*, 1061. (b) Nicolau, Y. F.; Menard, J. C. *J. Cryst. Growth* **1988**, *92*, 128. (c) Nicolau, Y. F.; Dupuy, M.; Brunel, M. *J. Electrochem. Soc.* **1990**, *137*, 2915. (d) Nicolau, Y. F.; Menard, J. C. *J. Appl. Electrochem.* **1990**, *20*, 1063. (e) Nicolau, Y. F.; Menard, J. C. *J. Colloid Interface Sci.* **1992**, *148*, 551.
(13) Ichinose, I.; Senzu, H.; Kunitake, T. *Chem. Mater.* **1997**, *9*, 1296.
(14) Fang, M.; Kim, C. H.; Martin, B. R.; Mallouk, T. E. *J. Nanoparticle Res.* **1999**, *1*, 43.
(15) (a) Gregory, B. W.; Stickney, J. L. *J. Electroanal. Chem.* **1991**, *300*, 543. (b) Suggs, D. W.; Villegas, I.; Gregory, B. W.; Stickney, J. L. *J. Vac. Sci. Technol. A* **1992**, *10*, 886. (c) Colletti, L. P.; Teklay, D.; Stickney, J. *J. Electroanal. Chem.* **1994**, *369*, 145. (d) Huang, B. M.; Colletti, L. P.; Gregory, B. W.; Anderson, J. L.; Stickney, J. L. *J. Electrochem. Soc.* **1995**, *142*, 3007.
(16) Tomkiewicz, M.; Ling, I.; Parsons, W. S. *J. Electrochem Soc.* **1982**, *129*, 2016.
(17) Mirley, C.; Koberstein, J. *Langmuir* **1995**, *11*, 1049.
(18) Kalachev, A.; Mathauer, K., Hohne, U.; Wegner, G. *Thin Solid Films* **1993**, *228*, 307.
(19) Moriguchi, I.; Maeda, H.; Taraoka, Y.; Kagawa, S. *J. Am. Chem. Soc.* **1995**, *117*, 1139.
(20) Suntola, T. *Mater. Sci. Rep.* **1989**, *4*, 261.
(21) Katada, N.; Niwa, M. *Chem. Vap. Deposition* **1996**, *2*, 125.
(22) Garlic, G.; Gibson, A. *J. Opt. Soc. Am.* **1949**, *39*, 935.
(23) Ohring, M. *The Materials Science of Thin Films*; Academic: San Diego, 1992.
(24) McClean, I.; Thomas, C. *Semicond. Sci. Technol.* **1992**, *7*, 1394.
(25) Jin, C.; Luttmer, J.; Smith, D.; Ramos, T. *MRS Bull.* **1997**, *22*, 10, 39.
(26) Green, W. H.; Le, K. P.; Grey, J.; Au, T. T.; Sailor, M. J. *Science* **1997**, *276*, 1826.

immersing the Si∧∧NH_2 substrate in the same $Zn(OAc)_2$ solution and aqueous NaOH solution (4.5 mM), rinsing and drying in the same way. For all three types of films, rinsing with water was done carefully, using a water stream directed parallel to the surface for 1 min. Experiments with longer rinsing times showed that they did not significantly affect the ellipsometric thickness of the films.

SiO_2 films were prepared by immersing the Si−OH substrate in a solution of $SiCl_4$ in CCl_4 (175 mM) for 2 min followed by rinsing with CCl_4 and methanol, and then drying in a stream of Ar. The substrate was then immersed in water for 1 min and dried in Ar.

By repeating these two-step adsorption cycles, multilayer films were synthesized. Each adsorption cycle was followed by ellipsometric measurements.

Characterization. Ellipsometric measurements were made with a Gaertner Scientific Corp. model L2W26D rotating polarizer ellipsometer. Si substrates were dried in an argon stream prior to the measurements. An analyzing wavelength of 632 nm was used. The film thickness of the multilayers was calculated using the Si refractive indices, $n_s = 3.875$ and $k_s = -0.018$, determined from a blank sample. The real and imaginary parts of the refractive index of the films were taken as 1.60 and zero, respectively. The value 1.60 was chosen smaller than that for bulk ZnS (2.36) and ZnO (2.02), assuming that the density of as-prepared films would be significantly less than that of the bulk crystalline compounds, as was shown for TiO_2 films in ref 13.

Atomic force microscopy (AFM) images of the multilayers deposited on Si substrates were obtained with a Digital Instruments Nanoscope IIIa in tapping mode using a 3045 JVW piezo tube scanner. The 125 μm etched Si cantilevers had a resonant frequency between 250 and 325 kHz and the oscillation frequency for scanning was set to ∼0.1−3 kHz below resonance. Typical images were obtained with line scan rates of 2 Hz while collecting 256 × 256 pixel samples.

Transmission UV−visible absorption spectra were obtained from the films deposited on quartz substrates with a Hewlett-Packard diode array HP8452A spectrometer.

Steady-state emission spectra were recorded with a SPEX Fluorolog 1680 0.22 m double monochromator fluorimeter using a front face illumination and collection geometry. The emission spectra were corrected for the instrument response as they were obtained.

X-ray photoelectron spectra (XPS) were obtained using Kratos Series 800 spectrometer with $h\nu = 1253.6$ eV and a 4 × 6 mm^2 analyzing window. The accuracy of measured core level binding energies (E_b) was ±0.1 eV.

Results and Discussion

Film Growth. The film growth can be schematically described by the following surface reaction sequences:

$$\text{Si}-\text{OH} \xrightarrow{Zn^{2+},\ OAc^-} \text{Si}-\text{O}-\text{Zn}(H_2O)_x(OAc)_y \xrightarrow{S^{2-}} \text{Si}-\text{O}-\text{Zn}-\text{S} \xrightarrow{Zn^{2+},\ OAc^-} \text{Si}-\text{O}-\text{Zn}-\text{S}-\text{Zn}(H_2O)_x(OAc)_y \text{ etc.} \quad \text{(I)}$$

$$\text{Si}\wedge\wedge\text{NH}_2 \xrightarrow{Zn^{2+},\ OAc^-} \text{Si}\wedge\wedge(NH_2)\text{Zn}(H_2O)_x(OAc)_y \xrightarrow{OH^-} \text{Si}\wedge\wedge(NH_2)\text{Zn}-\text{OH} \xrightarrow{Zn^{2+},\ OAc^-} \text{Si}\wedge\wedge(NH_2)\text{Zn}-\text{O}-\text{Zn}(H_2O)_x(OAc)_y \text{ etc.} \quad \text{(II)}$$

$$\text{Si}-\text{OH} \xrightarrow{SiCl_4} \text{Si}-\text{O}-\text{Si}-\text{Cl} \xrightarrow{H_2O} \text{Si}-\text{O}-\text{Si}-\text{OH etc.} \quad \text{(III)}$$

In the aqueous reaction sequences I and II, it is assumed that the weakly coordinating acetate ions are easily displaced as ligands for Zn^{2+} or Mn^{2+} by the more strongly coordinating OH^- or S^{2-} anions. The first association constant of OAc^- with Zn^{2+} is on the order of 10 M^{-1}, and at the concentrations of OAc^- used in these experments, one might expect to find both coordinated OAc^- and H_2O on the surface. This is borne out by XPS analysis of the films (see below). The binding of Zn^{2+} and Mn^{2+} ions to surface Si−OH groups (sequence I) is expected to be quite weak. On the other hand, alkylamines (sequence II) are relatively good ligands for both metal ions, with stepwise association constants in the range of 10^2−10^3 M^{-1}.[27] Covalent bond-forming reactions such as those in sequence III are generally assumed to be irreversible in SSG.[13]

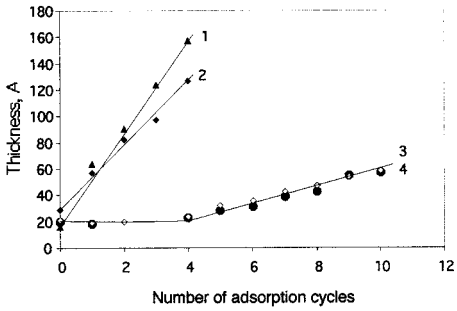

Figure 1. Ellipsometric thickness data for the Si−OH/SiO_2 (1), Si∧∧NH_2/ZnO (2), Si−OH/ZnS (3), and Si−OH/(Zn,Mn)S (4) films.

Ellipsometry. The growth of the films was monitored by ellipsometric measurements, and the data are shown in Figure 1. There is no noticeable growth of the Si−OH/ZnS and Si−OH/(Zn,Mn)S films during the first three two-step adsorption cycles. However, after the fourth cycle the films thickness plots become linear. This linearity indicates that on average the same amount of material is deposited in each adsorption cycle. The average increase in film thickness per layer is 6.2 and 5.7 Å for the Si−OH/ZnS and Si−OH/(Zn,Mn)S films, respectively. In contrast, for the both oxide films, Si−OH/SiO_2 and Si−NH_2/ZnO, good linearity in the films thickness plots is observed starting from the first adsorption cycle. The average increase in film thickness per each cycle is 24.5 and 35 Å for the Si−NH_2/ZnO and Si−OH/SiO_2 films, respectively. The average increments per cycle for the oxide films are substantially greater than might be expected for a monolayer-by-monolayer growth process. Different oxide films give thinner or thicker films by SSG. The ZnO and SiO_2 films prepared here have average thicknesses per cycle that are within the range of oxide films previously measured by quartz crystal microbalance (4−50 Å[13]) and X-ray diffraction (4.5 Å[14]) techniques.

We note that previously reported SSG techniques for the oxide film preparation[13,14] employed organic solutions of metal−organic precursors. In those cases, special care had to be taken to keep the reaction environment strictly anhydrous, since alkoxide precursors are sensitive to hydrolysis and subsequent polymerization. In the case of ZnO and ZnS film synthesis from the acetate precursor, aqueous media were preferable. No film growth was observed when a solution of $Zn(OAc)_2$ in EtOH/HOAc was used (although TiO_2 films were successfully deposited from a solution of $TiO(acac)_2$

(27) Sillen, L. G.; Martell, A. E. *Stablility Constants of Metal-Ion Complexes*; Special Publications 17 and 25; The Chemical Society: London, 1964 and 1971.

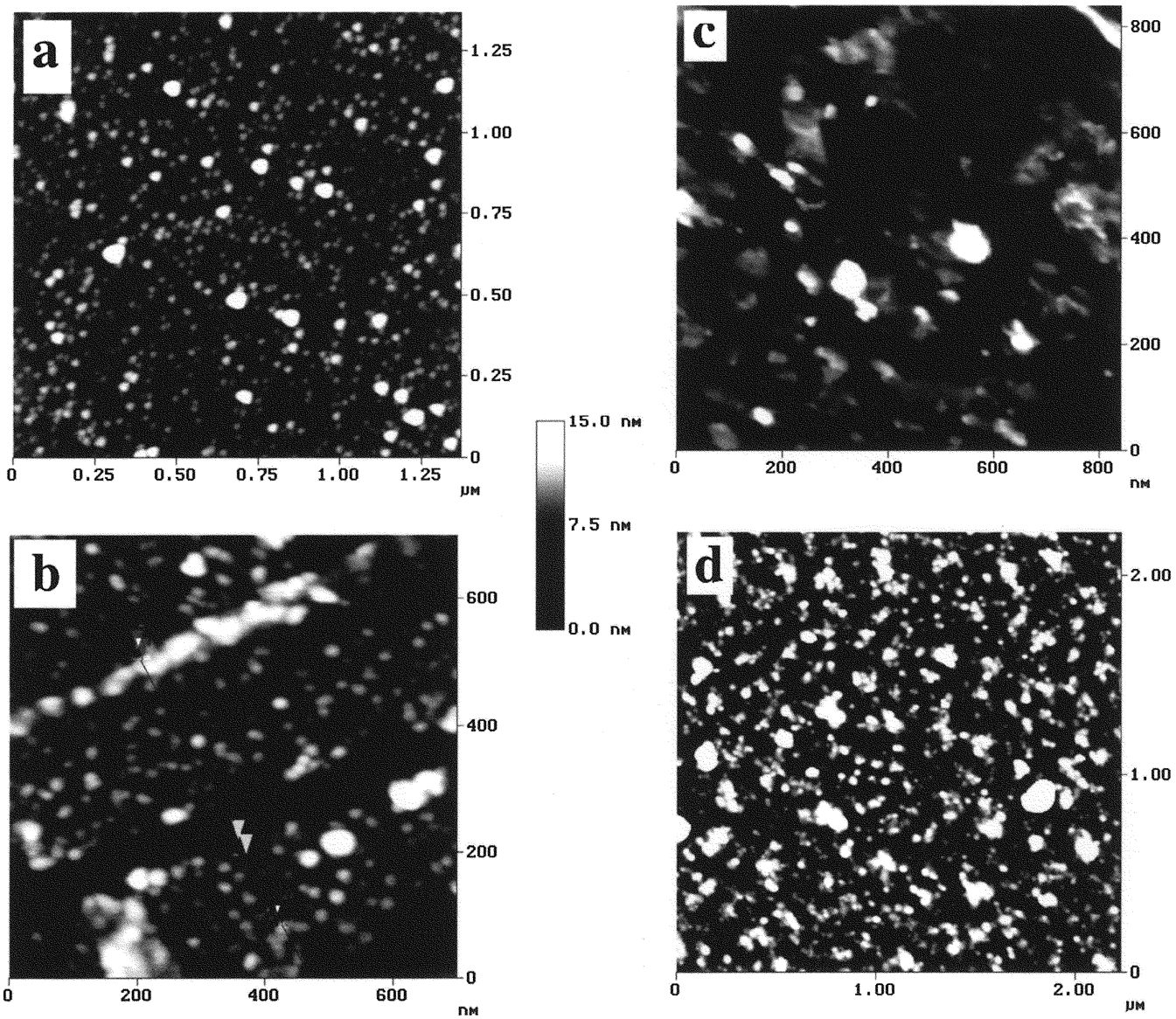

Figure 2. Tapping-mode AFM images of (a) Si−OH/ZnS film deposited in 10 adsorption cycles, (b) Si−OH/(Zn,Mn)S film deposited in 10 adsorption cycles, (c) Si∧∧NH_2/ZnO film deposited in 4 adsorption cycles, and (d) Si−OH/SiO_2 film deposited in 4 adsorption cycles.

in MeOH/HOAc[13]). Apparently, there is sufficiently strong coordination of Zn^{2+} ions in EtOH/HOAc that the surface interaction is weak or easily reversed in the washing step. It should also be noted that no ZnO film formation was achieved on Si−OH substrates during six adsorption cycles. This implies that the ZnO film growth requires stronger linking of Zn^{2+} ions to the surface via coordination to NH_2 groups. An essential condition for a successful SSG process is that the binding of the chemisorbed monolayer is irreversible, or sufficiently strong to prevent desorption in the subsequent rinsing/activation step. Thus proper choice of film growth parameters, such as the chemical composition of the surface and solvent used, is necessary for the successful formation of surface-bound nanoparticles. It has been shown previously that the chemical composition of the anion in a metal salt precursor and its concentration affect the rate of film growth.[12] Similarly, temperature has been shown to be an important factor in controlling the kinetics of SSG reactions[13] and the thermodynamics of metal coordination reactions on surfaces.[28]

Morphology of the Films. Typical AFM images of the sulfide and oxide films prepared are shown in Figure 2a−d. The images of both Si−OH/ZnS and Si−OH/(Zn,-Mn)S films grown in 10 adsorption cycles (Figure 2 a,b) reveal close-packed layers of well-resolved rounded features about 10−30 nm in diameter and 4−9 nm in height. CdS layers deposited by SSG on TiO_2 surfaces had similar morphologies.[11] For the Si−OH/(Zn,Mn)S film (Figure 2b) a part of the image containing the uncovered substrate surface was selected in order to estimate the approximate film thickness. The thickness is about 4.2 nm, which is in good agreement with the average thickness found by ellipsometry, 4 nm (Figure 1.4). This value is also consistent with the height of the rounded features and suggests crystal growth immediately on the Si−OH surface. The surface coverage is estimated to be ∼90% and 75% for the Si−OH/ZnS and Si−OH/(Zn,Mn)S films, respectively. An image of

(28) Bell, C. M.; Arendt, M. F.; Gomez, L.; Schmehl, R. H.; Mallouk, T. E. *J. Am. Chem. Soc.* **1994**, *116*, 8374.

the Si−OH/ZnS film deposited in five adsorption cycles (not shown) also shows evenly distributed rounded features of approximately the same diameter, but their average height is lower (1−7 nm). The surface coverage in the latter case was estimated at about 80%. These data suggest that the sulfide nanoparticles form on the surface from well-separated crystal nuclei, rather than from a saturated chemisorbed monolayer, as is normally the case in ALE,[20] or in ECALE films nucleated by underpotential deposition of one ion.[15,16] The metal sulfide particle growth in the lateral direction is almost completed in about five adsorption cycles, after which growth in vertical direction prevails.

The image of the Si−OH/SiO_2 film deposited in four adsorption cycles (Figure 2d) shows densely a packed particle layer completely covering the surface. Such a morphology is consistent with a high density of nucleation sites for the first layer, which follows from the high density of Si−OH sites and the formation of strong covalent Si−O−Si bonds from the surface reaction of $SiCl_4$. The film surface contains features of about 30−60 nm in diameter, which form aggregates. The average roughness of the film is about 3.2 nm.

The surface morphology of the Si∧∧NH_2/ZnO film grown in four adsorption cycles is quite different from those described above. No well-resolved rounded features are observed. Instead, the film consists of extended (50−500 nm) and rather flat separate islands of different thickness, which cover about 70% of the surface. Figure 2c shows an area of the surface that is covered with relatively thin (3−5 nm) and quite smooth islands. The average roughness of these islands is about 0.85 nm.

Although the mechanism of the SSG film growth process is still not understood in detail, the significant difference in the morphology of the ZnO film and the other films makes us believe in the existence of at least two possible descriptions of the main events of the films growth. The first one, which is consistent with the formation of three-dimensional, rounded features, involves continuous particle growth from nuclei, and approximately follows the Ostwald model for colloids: $(ZnS)_{m+n} + Zn^{2+} + S^{2-} \rightarrow (ZnS)_{m+n+1}$ etc. In this case, the strength of bonds within the particle is greater than that of the bonds anchoring the particle to the substrate. This is the case for ZnS, and also apparently for SiO_2.

In the case of the ZnO films, the formation of islands is consistent with the formation of ZnO at islands of Si∧∧NH_2 on an otherwise unreactive surface, or with growth from sparse amine nucleation sites with the primary growth direction being horizontal. On the basis of our experience with priming layers of organosilanes, we favor the former explanation. That is, the priming monolayer formed from 4-((dimethylmethoxy)silyl)butylamine is relatively patchy, and it nucleates the growth of the ZnO film. There are two possible explanations for the unusual smoothness of the ZnO films grown on the amine islands. The first one involves strong coordination of Zn^{2+} ions by the amine monolayer. Subsequent reaction with base converts this to a surface Zn−OH film, which coordinates more Zn^{2+} ions in the next adsorption cycle, etc., to form a smooth film. This model assumes dense packing of the amine groups within the surface islands, allowing the formation of continuous surface Zn−O−Zn−O surface layers. In this case one might expect that the films formed would be dense, and perhaps would show a preferred crystallographic orientation. However, it is more likely that the tethered butylamine groups within the islands are disordered and disposed at a distance from each other, in which case the nucleation of separate $(ZnO)_n$ primary clusters would occur. A smooth film could result if these small clusters have some lateral mobility on the amine surface and can aggregate to form a film. In this case, one would expect a disordered or polycrystalline film. We observed that the ZnO film could be partially removed from the surface if the washing steps were not done carefully. This suggests that the second model is probably operative. Unfortunately, the ZnO films shown in Figure 2 were too thin to obtain Bragg diffraction peaks by X-ray diffraction, which might have distinguished between the two models for smooth film growth.

Chemical Composition of the Films. The surface chemical compositions of the Si∧∧NH_2/ZnO, Si−OH/ZnS and Si−OH/(Zn,Mn)S films were determined by XPS. The position of the Zn $p_{3/2}$ line in the spectra of the ZnO film (1022.5 eV) and both of the ZnS-containing films (1021.8 eV) is characteristic of bulk ZnO and ZnS respectively.[29]

For Si−OH/(Zn,Mn)S film, the Mn_{2p} XPS spectrum reveals a photoelectron line at 639.8 eV, which is accompanied by two shake-up satellites at 651.3 and 657.1 eV. This spectrum is characteristic of isolated paramagnetic Mn^{2+}.[29] The Zn:Mn:S surface ratio was found to be 1:0.064:0.61 (see Table). It is interesting to note that Zn:Mn ratio in the film is about 3 times higher than in starting solution, consistent with the much lower solubility product of ZnS (4.5×10^{-24}) relative to MnS (3×10^{-13}).[30]

In each of the three XPS spectra, the intense C_{1s} line from adventitious carbon is asymmetrical and has a shoulder at 288.1−288.3 eV, indicating the presence of O−C═O bonds, and hence acetate groups.[29] By integrating the area of the deconvoluted peaks, the approximate percentages of acetate groups in the films were determined to be 3.3%, 4.8%, and 3.1% for Si∧∧NH_2/ZnO, Si−OH/ZnS, and Si−OH/(Zn,Mn)S, respectively. Residual precursor molecules suggest incomplete sulfidization or hydrolysis. Similar residual ligands have been detected in ZnO colloids,[31] metal oxide films prepared by SSG[12] and in ZnS nanoparticles grown on SiO_2 by sonochemical reactions.[32]

An Si_{2p} line, which originates from the uncovered substrate, is observed for all the samples. Its envelope exhibits two distinct features: bulk silicon at 99.1 eV and oxidized silicon at 102.2−102.9 eV. The latter peak appears at lower energy than that observed for SiO_2 (103.3−103.7 eV),[29] and is characteristic of the Si(+4) oxidation state in different inorganic environments (e.g., SiO_2, SiO_x ($x < 2$), and $SiO_x(OH)_y$). The approximate percentages of the oxidized silicon species in the samples

(29) Moulder, J. F.; Stickle, W. F.; Sobol, P. E.; Bomben, K. D. *Handbook of X-ray Photoelectron Spectroscopy*; Perkin-Elmer Co., Phys. Electron. Div.: Minnesota.

(30) Meites, L. *Handbook of Analytical Chemistry*; McGraw-Hill: New York, 1963; pp 1−13.

(31) Spanhel, L.; Anderson, M. A. *J. Am. Chem. Soc.* **1991**, *113*, 2826.

(32) Dhas, N. A.; Zaban, A.; Gedanken, A. *Chem. Mater.* **1999**, *11*, 806.

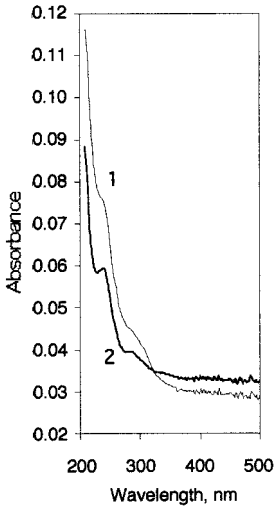

Figure 3. Transmission UV−visible spectra of ZnS (1) and (Zn,Mn)S (2) films deposited in 10 adsorption cycles on quartz slides.

Table 1. Relative Integrated XPS Peak Areas, Corrected for Atomic Sensitivity, for Si∧∧NH_2/ZnO and Si−OH/(Zn,Mn)S Films

element	Si−NH_2/ZnO	Si−OH/(Zn,Mn)S
Si	9.14	31.35
S		5.46
C	56.78	31.14
N	0.79	
O	22.79	22.42
Mn		0.58
Zn	10.5	9.0

were 3.7%, 2.4%, and 7.4% for Si∧∧NH_2/ZnO, Si−OH/ZnS, and Si−OH/(Zn,Mn)S, respectively. The uncertain composition of the oxidized silicon species prevents an accurate determination of the Zn:O ratio in the Si∧∧NH_2/ZnO film. For the Si−OH/(Zn,Mn)S sample, the total oxygen content is roughly consistent with the oxygen included in the acetate groups and the oxidized silicon, which suggests no significant content of oxide in the semiconductor nanoparticle film (Table 1).

Optical Properties. UV−vis absorption spectra of ZnS and (Zn,Mn)S films deposited in five adsorption cycles on quartz slides (the surface of the quartz slides was first hydroxylated in the same way as the Si wafers) are shown in Figure 3. The ZnS film spectrum reveals a steep absorption edge at 240 nm and a shoulder at 270 nm, and is quite similar to spectra reported for ZnS colloids.[33] In the spectrum of the (Zn,Mn)S film, the steep absorption edge (245 nm) and shoulder (280 nm) are slightly red shifted, a shoulder at 330 nm appears from Mn^{2+}-based transitions. Band gap energies estimated from the spectra (5.17 and 5.07 eV for ZnS and (Zn,Mn)S, respectively) are consistent with quantum size effects, as expected from the small particle sizes observed by AFM.

The photoluminescence (PL) spectrum of the ZnS film excited a 290 nm displays a broad emission centered at 445 nm (Figure 4a). Photoluminescence in this spectral region is attributed to the presence of sulfur vacancies in the lattice, as previously found for ZnS colloids[33−35] and SiO_2/ZnS nanoparticles.[32] This emission results

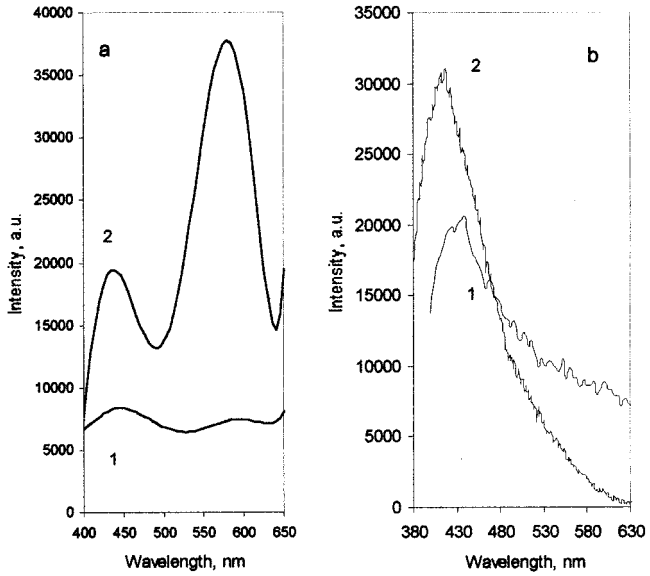

Figure 4. Photoluminescence spectra of (a) sulfide films Si−OH/ZnS (1) and Si−OH/(Zn,Mn)S (2) deposited in 10 adsorption cycles; (b) oxide films Si∧∧NH_2/ZnO (1) and Si−OH/SiO_2 (2) deposited in 4 adsorption cycles. Excitation wavelengths were 290 nm in (a) and 340 nm in (b).

from the recombination of photogenerated charge carriers in shallow traps.[33,34]

The PL spectrum of the (Zn,Mn)S film (Figure 4a) reveals blue-green and yellow emissions at about 438 and 580 nm. This Mn^{2+}-based yellow emission has been observed in the photoluminescence of doped ZnS:Mn nanoparticles[33,36,37] and assigned to the Mn^{2+} $^4T_1-^6A_1$ transition. It is known that the Mn^{2+} ion d electron states act as luminescent centers because of strong interaction with the s−p electronic states of the ZnS nanocrystals, which are excited by band gap absorption. The yellow emission in the PL spectrum of the (Zn,Mn)S film indicates the existence of an energy-transfer pathway that arises from electronic interaction in the (Zn,Mn)S clusters, and hence the introduction of Mn^{2+} ions into ZnS host lattice.

In the PL spectrum of the ZnO film, a broad emission centered at 440 nm is observed (Figure 4b). As has been previously found for ZnO colloids, the position of the emission peak is strongly dependent on particles size and falls within the range of 420−560 nm.[31,38,39] Freshly prepared ZnO sols exhibit blue emission, which changes to blue-green within 1 h.[39] Green emission around 450 nm is also observed in ZnO colloids prepared in alkaline alcohol solutions.[39] The emission band at 440 nm observed in our experiments implies that the ZnO film is composed of very small ZnO grains with a size close to that of colloidal particles in freshly prepared sols (∼3 nm[31]). This result is consistent with the smooth, featureless films observed in the AFM image. The broad emission spectra observed for both ZnS and ZnO nanoparticle films can be explained as follows. Photogenerated charge carriers, which have been trapped in

(33) Sooklal, K.; Cullum, B. S.; Angel, S. M.; Murphy, C. J. *J. Phys. Chem.* **1996**, *100*, 4551.
(34) Becker, W. G.; Bard, A. J. *J. Phys. Chem.* **1983**, *87*, 4888.
(35) Rabani, J. *J. Phys. Chem.* **1989**, *93*, 7707.
(36) Bhargava, R. N.; Gallagher, D. *Phys. Rev. Lett.* **1994**, *72*, 416.
(37) Igarashi, T.; Isobe, T.; Senna, M. *Phys. Rev. B* **1997**, *56*, 6444.
(38) Bahnemann, D. W.; Kormann, C.; Hoffmann, R. M. *J. Phys. Chem.* **1987**, *91*, 3789.
(39) Kamat, P. V.; Patrick, B. *J. Phys. Chem.* **1992**, *96*, 6829.

shallow and deep surface states, tunnel to each other to recombine. Emission from recombination of short-distance pairs (in shallow traps) appears at lower wavelength than that from long-distance pairs (in deep traps). Broad emission bands represent a superposition of the wide distribution of trap distances.[31]

The SiO_2 film shows a broad emission band centered at 415 nm when excited at 340 nm (Figure 4b). Photoluminescence in this spectral region is due to oxygen vacancies associated with electrons localized on the bridge oxygen atoms of siloxane linkages.[40]

Conclusions

We have shown that the surface sol−gel technique can be used to make ultrathin films of ZnS_x, Mn-doped ZnS_x, and ZnO_x nanoparticles from aqueous precursor solutions. The thickness of the films is controlled by the number of adsorption cycles, and dense coverage of the substrate can be achieved in 4−10 adsorption cycles. The coverage and morphology of the films depend on a number of factors, including the nature of surface priming layer and the choice of solvent and solutes. The optical properties of the films are similar to those of sol−gel nanoparticles in prepared in the liquid phase. For Mn-doped ZnS_x films, PL data show that Mn^{2+} ions are incorporated into the ZnS host lattice. The morphology of the thin films can be understood in terms of nucleation and growth phenomena, which depend on the relative strength of interactions of metal ions with the surface priming layer and with ligands introduced in the following adsorption cycle.

Acknowledgment. This work has in part been supported by Civilian Research and Development Foundation, USA, grant UC1-338. Work at The Pennsylvania State University was supported by National Science Foundation grant CHE-9529202. Instrumentation for AFM experiments was provided by National Science Foundation grant CHE-9626326.

CM990395P

(40) Eremenko, A.; Smirnova, N.; Samchuk, S.; Chuiko, A. *Colloids Surfaces* **1992**, *63*, 83.